

T-independent response mediated by oncolytic tanapoxvirus recombinants expressing interleukin-2 and monocyte chemoattractant protein-1 suppresses human triple negative breast tumors

Yogesh R. Suryawanashi¹ · Tiantian Zhang¹ · Helene M. Woyczeszcyk¹ · John Christie^{1,3} · Emily Byers^{1,4} · Steven Kohler¹ · Robert Eversole¹ · Charles Mackenzie² · Karim Essani¹ 

Received: 17 April 2017 / Accepted: 27 April 2017 / Published online: 2 May 2017
© Springer Science+Business Media New York 2017

Abstract Human triple negative breast cancer (TNBC) is an aggressive disease, associated with a high rate of recurrence and metastasis. Current therapeutics for TNBC are limited, highly toxic and show inconsistent efficacy due to a high degree of intra-tumoral and inter-tumoral heterogeneity. Oncolytic viruses (OVs) are an emerging treatment option for cancers. Several OVs are currently under investigation in preclinical and clinical settings. Here, we examine the oncolytic potential of two tanapoxvirus (TPV) recombinants expressing mouse monocyte chemoattractant protein (mMCP)-1 [also known as mCCL2] and mouse interleukin (mIL)-2, in human TNBC, in vitro and in vivo. Both wild-type (wt) TPV and TPV recombinants demonstrated efficient replicability in human TNBC cells and killed cancer cell efficiently in a dose-dependent manner in vitro. TPV/ Δ 66R/mCCL2 and TPV/ Δ 66R/mIL-2 expressing mCCL2 and mIL-2, respectively, suppressed the growth of MDA-MB-231 tumor xenografts in nude mice significantly, as compared to the mock-injected tumors. Histological analysis of tumors showed areas of viable tumor cells, necrotic foci and immune cell accumulation in virus-treated tumors. Moreover, TPV/

Δ 66R/mIL-2-treated tumors showed a deep infiltration of mononuclear immune cells into the tumor capsule and focal cell death in tumors. In conclusion, TPV recombinants expressing mCCL2 and mIL-2 showed a significant therapeutic effect in MDA-MB-231 tumor xenografts, in nude mice through induction of potent antitumor immune responses. Considering the oncolytic potency of armed oncolytic TPV recombinants expressing mCCL2 and mIL-2 in an experimental nude mouse model, these viruses merit further investigation as alternative treatment options for human breast cancer.

Keywords Tanapoxvirus · Oncolytic virus · Triple negative breast cancer · Antitumor macrophages · Monocyte chemoattractant protein-1/CCL2 · Interleukin-2

Introduction

Breast cancer (BC) is one of the leading causes of cancer-related mortality among women in the USA [1]. Molecular heterogeneity among BC subtypes and severe toxicity associated with the standard chemotherapy and radiotherapy are some of the major hurdles in optimizing the treatment strategy for BC [2–4]. Triple negative breast cancer (TNBC), a subtype of BC is associated with poor prognosis owing to its aggressive nature and early metastasis [5]. Hormone-based therapies are ineffective against TNBC due to the absence of estrogen and progesterone receptors on these cells [6]. Chemotherapy is still a standard treatment used for TNBC, but there is a high rate of recurrence among these patients due to subsequent development of chemo-resistance [7]. Limited treatment options and lack of common therapeutic targets in TNBC have created a dire need for newer treatment options [7].

✉ Karim Essani
karim.essani@wmich.edu

¹ Laboratory of Virology, Department of Biological Sciences, Western Michigan University, Kalamazoo, MI 49008-5410, USA

² Department of Pathology, Liverpool School of Tropical Medicine, Pembroke Place, Liverpool L3 5QA, UK

³ Present Address: The Biodesign Institute, Arizona State University, Tempe, AZ, USA

⁴ Present Address: General Toxicology, MPI Research, Mattawan, MI, USA

Replication competent oncolytic viruses (OVs) can kill cancer cells directly through postinfection cell lysis and concomitantly target them indirectly through activation of comprehensive anticancer immunity. Oncolytic herpes virus (T-VEC), expressing human granulocyte monocyte colony-stimulating factor is the first OV approved by the Food and Drug Administration (FDA) for human melanoma treatment in the USA [8]. Several OVs, including oncolytic poxviruses in clinical trials for the treatment of breast and other cancer types have shown promising results [9, 10]. An inherent advantage with poxviruses is that cancer cells are more permissive to poxviruses due to defective antiviral innate immune response pathways, unlike the non-transformed cells which respond quickly to poxvirus infection and impede viral replication [11].

Tanapoxvirus (TPV) is classified in the family *Poxviridae* and is a member of genus *Yatapoxvirus*. TPV is a suitable OV candidate as most humans do not have a preexisting immunity, since it is geographically restricted to equatorial Africa and does not show a cross-reactivity with other poxviruses, including vaccinia virus [12, 13]. In the absence of antiviral immunological tolerance, oncolytic TPV is a useful addition to a large bank of antigenically distinct OVs that can be used in a serial manner to avoid a potential loss of therapeutic efficacy of OVs [12]. TPV also scores well for safety and ease of use, as it causes a mild, self-limiting febrile illness in humans, does not spread from individual to individual, and has a large viral genome (around 145 kb) that can carry multiple therapeutic transgenes [12, 14]. Our laboratory has reported earlier the therapeutic efficacy of TPV in treating human colorectal cancer and melanoma in a nude mouse model [15, 16].

Deletion of the viral *thymidine kinase* (*TK*) gene to enhance preferential replication of OVs in cancer cells that have abundant pools of thymidine triphosphate (TTP), is a commonly used strategy when designing OVs [17]. In this study, we tested the oncolytic potential of TPV recombinants with *TK(66R)* gene knocked out and expressing mouse monocyte chemoattractant protein (mMCP-1/mCCL2) and mouse interleukin (mIL)-2, in human TNBC. The MCP-1, also known as CCL2, is a chemotactic factor that recruits monocytes, T lymphocytes, natural killer (NK) cells, dendritic cells and mast cells to the site of inflammation [18–20]. CCL2 plays a pleiotropic role in the immune response against cancer cells as it can invoke antitumor immune response through activation of tumoricidal macrophages [21]. It also promotes tumor cell growth, survival, invasion, metastasis, deleterious peritumoral inflammation and tumor angiogenesis [22]. CCL2 has been effective in treating human pancreatic cancer and murine neuroblastoma [23, 24]. IL-2 is known as a growth factor for T lymphocytes and NK cells that can also promote differentiation, growth and maturation of T cells and

activation of antitumor macrophages [25–27]. IL-2 has played an important role in developing chimeric antigen receptor (CAR) T cells [28]. In addition to interferon (IFN)- α , IL-2 is the only cytokine approved for cancer treatment in adults by the FDA [29].

We tested the therapeutic potency of TPV recombinants in athymic nude mice that have a competent innate immune system. Although athymic nude mice are deficient in peripheral T cells, other immune cells such as macrophages, NK cells, granulocytes, B cells and dendritic cells are immunologically competent [30]. Moreover, this is a compensatory increase in the number of antitumor macrophages and NK cells in athymic nude mice [30]. Among the mononuclear cells present in nude mice, macrophages seem to be predominant [31]. Both CCL2 and IL-2 are known to play critical roles in activation of innate immune responses through macrophages, NK cells, dendritic cells, and mast cells. Herein, we used athymic nude mice to study the therapeutic potential of TPV recombinants expressing CCL2 and IL-2 which is a bona fide method to test the innate immune responses induced by these virotherapeutics and has been commonly used in studies assessing the efficacy of cancer immunotherapeutics.

Our results indicate that TPV recombinants expressing mCCL2 and mIL-2 were most effective in suppressing the growth of MDA-MB-231 xenografts in nude mice. Histological analyses of tumors also support the notion that mononuclear immune cell response against tumor played a role in tumor egression, where TPV recombinant expressing mIL-2 showed a significant effect. Significantly higher number of mononuclear cells was detected in the capsules of TPV/ Δ 66R/mIL-2-treated tumors, compared to other treatment groups.

Materials and methods

Cells, viruses and reagents

Owl monkey kidney (OMK) cells, human fetal lung fibroblasts (WI-38), and human triple negative breast cancer cell lines (MDA-MB231, MDA-MB157, MDA-MB436) were purchased from American Type Culture Collection (ATCC, Rockville, MD, USA). OMK and WI-38 cells were cultured in an atmosphere of 5% CO₂ in growth media consisting of Eagle's minimum essential medium (EMEM), supplemented with 10% fetal bovine serum (FBS) (v/v%), 100 U/ml penicillin, and 100 μ g/ml streptomycin at 37 °C. MDA-MB231, MDA-MB157, and MDA-MB436 cells were cultured in Leibovitz's (L-15) growth medium, supplemented with 10% FBS (v/v%), 100 U/ml penicillin, and 100 μ g/ml streptomycin at 37 °C without CO₂. L-15 was additionally supplemented with

10 µg/ml insulin and 16 µg/ml glutathione for MDA-MB436 cells. All cell lines were cultured in maintenance medium following virus infection. The maintenance media had lower FBS content [2% (v/v)] but was otherwise identical to the growth medium. Wild-type (wt)-TPV [Kenya] (a gift from late Dr. Joseph Esposito, Centers for Disease Control, Atlanta, GA, USA) was used to generate a panel of TPV recombinants. Generation of TPV/Δ66R, TPV/Δ66R/mCCL2 and TPV/Δ66R/mIL-2 has been described earlier [15, 32]. Expression of *mIL-2* and *mCCL2* transgenes was confirmed by western blot analysis and ELISA assay, respectively, and *TK* gene deletion was confirmed by PCR [15, 32].

Virus replication assay

All viruses were amplified in OMK cells and concentrated to 100× using ultracentrifugation (type 45Ti rotor at 186,000×g for 90 min), and the titer of the resultant viruses was determined on OMK cell monolayers in 6-well plates as described earlier [33]. For the viral replication assay, WI-38 and human TNBC cells were plated in 12-well plates at 5×10^4 cells per well density and infected with wtTPV or one of the TPV recombinants at 0.1 multiplicity of infection (MOI), as described earlier [33]. Infected cultures were harvested at 48, 96 and 240 h postinfection (hpi). To release the intracellular virus, cells were scraped, centrifuged (500×g for 10 min) and resuspended in sterile deionized water and subjected to 3 cycles of freezing and thawing. Samples were pooled with the supernatant to bring the total volume to 1 ml, followed by a mixing and sonication on ice for 30 s. Total virus yield was determined by a plaque assay described earlier [33]. All experiments were independently repeated 3 times.

Cell viability assay

Human TNBC cell lines (MDA-MB-231, MDA-MB-157, MDA-MB-436) were cultured in 96-well plates at a density of 1×10^3 cells per well and incubated overnight in L-15 medium with 10% FBS at 37 °C without CO₂. The total live cell numbers in each well were determined using an improved Neubauer hemocytometer after trypsinizing the representative wells and staining cells with 0.2% (wt/vol) trypan blue in a phosphate buffer saline (PBS). Cells were infected with wtTPV or one of the TPV recombinants at 0.1 and/or 5 MOI and incubated in L-15 medium with 2% FBS. A formazan dye approach was then used to determine cell viability at 96 and/or 240 hpi. A cell counting kit (CCK-8) (Sigma Aldrich, St. Louis, MO, USA) was used following the manufacturer's protocol. Cells were then incubated with the CCK-8 kit formazan dye for 2 h before measuring the absorbance of 450 nm with an ELISA plate reader

(BioTech Epoch). Results were obtained after replicating the experiment 3 times independently.

Preparation of conditioned medium

OMK cells were plated in 250 cm² tissue culture flask in EMEM with 10% FBS for 24 h and infected with either TPV/Δ66R or TPV/Δ66R/mCCL2 at 5 MOI and incubated in EMEM maintenance with 2% FBS, and cultures were harvested at 8-day postinfection when most of the cell monolayers were destroyed. Cultures were subjected to ultracentrifugation (type 45Ti rotor at 186,000×g for 90 min), and supernatants were collected and passed through 0.22 µm filter to remove virus particles and used as conditioned medium. OMK cells incubated with the conditioned medium to confirm the absence of TPV. We have referred to the conditioned media prepared after infection with TPV/Δ66R and TPV/Δ66R/mCCL2 as control conditioned medium and CCL2 conditioned medium, respectively.

Animals

Athymic male nude mice were purchased at 4 weeks age and acclimated for a week before beginning the experiments. Animals were housed, and treatments were carried out following the protocols approved by the Institutional Animal Care and Use Committee of Western Michigan University (IACUC protocol number 13-07-01).

Cell survival assay

The MDA-MB-231 cells were plated in 96-well plates (5×10^4 cells per well) in 100 µl of L-15 with 10% FBS. Cells were treated without or with recombinant (r) mCCL2 (10, 100 or 100,000 ng/ml) [R&D systems, Minneapolis, MN] in L-15 medium for 24 h at 37 °C with no CO₂. Alternatively, MDA-MB-231 cells were incubated with either control conditioned medium or CCL2 conditioned medium (100, 10 or 1 µl) for 24 h at 37 °C in 5% CO₂. Cell viability was assessed as above using a CCK-8 kit, following the manufacturer's recommended protocol.

Virotherapy of human TNBC xenografts in nude mice

Tumor xenografts were induced by injecting MDA-MB-231 cells (5×10^6) resuspended in 100 µl of sterile PBS, subcutaneously (SC) on the dorsal surface, in 5-week-old, athymic male nude mice (NCI:Hsd:athymic nude-*Foxn1*tm, Envigo, Indianapolis, IN). Cell viability was tested at the end of injection using trypan blue, as described earlier, to ensure the viable cell count at the time of injection which

showed that over 90% cells retained viability. Once visible, tumor volumes were measured with a digital caliper using the formula $\text{volume} = (\pi/6) \times (\text{length}) \times (\text{width}) \times (\text{height})$ in mm^3 . Once the tumor size reached the volume of $50 \pm 5 \text{ mm}^3$, mice were assigned randomly to a control or one of the treatment groups. Tumor xenografts in the treatment groups were injected with a single dose of 5×10^6 pfu of virus, suspended in 100 μl of EMEM maintenance medium (vehicle), intratumorally (IT). Tumor xenografts in the control group were injected IT, with 100 μl of vehicle only. Tumor volumes were measured every 2 days after virotherapy treatment over a 36-day period. Tumors and lung tissue samples were removed and preserved for histopathological analysis, on day 36 after virotherapy. Majority of animals in the mock group had met IACUC criteria for euthanasia by 36-day post-virotherapy, hence determined as the end point of tumor virotherapy experiment.

Tissue preparation and histological analyses

Tumor xenografts were removed from the animals and placed in 10% formalin for over 48 h and then moved to 60% ethanol for storage until processing. At processing the tumors were bisected through the longest plane and H&E stained paraffin sections prepared. These sections were examined for the following characteristics: overall size of the tumor section, nature, and form of the neoplastic cell, mitotic index (number of mitoses per 100 cells, counted at 100 \times magnification, assessing at least 10 fields of intact tumor cells), the presence of dead or degenerating cells, the presence of host inflammatory cells, and the morphological nature of the capsular region surrounding the masses. Except for the mitotic index, these characteristics were assessed using a semiquantitative system (normal –, minor changes +, moderate changes ++, extensive changes +++). The main changes recorded included the presence of fibrosis, inflammatory cells (and their morphological nature) and the invasion of host inflammatory cells in the main body of the tumor itself.

Statistical analysis

To compare the cell viability, the percent of viable cells were compared against the positive control for each cell line using a one-way analysis of variance (ANOVA) test with a post hoc analysis using Tukey's procedure, (significance level set to $p < 0.05$ with $n = 3$). The growth of the tumor xenografts was compared using a Mann–Whitney U test with each treatment group compared against the mock-treated control. Each time point was analyzed separately with the $n = 5$ mice per group and a significance set to $p < 0.05$.

For analysis of tumor growth rate, the instantaneous rate of tumor growth (k) was estimated as $k = \log(\text{Vol}_t/\text{Vol}_0)/t$ for each mouse, where Vol_t and Vol_0 are the tumor volume on day t and day 0, respectively. We then used the one-way ANOVA to test whether tumor growth rate (k) differed among treatments. We used planned contrasts to test whether tumor growth rate in the TPV/ Δ 66R treatment differed from that in either the TPV/ Δ 66R/mCCL2 or TPV/ Δ 66R/mIL-2 treatments. All analyses were performed using R 3.3.2.

Results

Replication assay of TPV recombinants in human triple negative breast cancer cells

To test the replication efficacy of TPV recombinants, MDA-MB-231, MBA-MB-436 and MBA-MB-157 cells were infected with wtTPV or TPV/ Δ 66R or TPV/ Δ 66R/mCCL2 or TPV/ Δ 66R/mIL-2 at 0.1 MOI. In this experimental setting wtTPV was used as a control virus, and WI-38 was a control cell line. Standard plaque assays were performed for all samples to determine the viral titers at different time points (48, 96 and 240 hpi) during the course of infection (Fig. 1). Virus titers reached the maximum for all TPV recombinants, at 96 hpi in all human TNBC cell lines. Among human TNBC cell lines, the highest titer for wtTPV was obtained for MDA-MB-436 (5.77×10^4) at 96 hpi and showed more than 15-fold increase in the virus titer between 48 and 96 hpi. However, wtTPV replicated equally well in all human TNBC cell lines as the virus yield from MDA-MB-231 (4.94×10^4) and MBA-MB-157 (4.59×10^4) did not differ significantly from MDA-MB-436, at 96 hpi. Replication of TPV/ Δ 66R was slower as compared to wtTPV in WI-38 and all human TNBC cell lines where the virus titers of TPV/ Δ 66R were significantly lower than wtTPV at 96 hpi ($p < 0.5$). The highest titer of TPV/ Δ 66R was found in MDA-MB-231 cells (2.97×10^4) among human TNBC cells at 96 hpi, which was fourfold increase from the viral titer 48 hpi. In addition, the highest titers for both TPV/ Δ 66R/mCCL2 (1.81×10^4) and TPV/ Δ 66R/mIL-2 (2.01×10^4) were calculated in MDA-MB-231 cells at 96 hpi. The WI-38 cells supported TPV replication better than any of the human TNBC cells used in the replication assay but the replication pattern of TPV was similar in all cells, with virus titers reaching the maximum level at 96 hpi. The total virus titers obtained from WI-38 cells were higher than any of the human TNBC cells at all three time points for all viruses. TPV recombinants engineered to express mCCL2 and mIL-2 showed an overall lower replication efficacy as compared to wtTPV, in both WI-38 and human TNBC cells but were

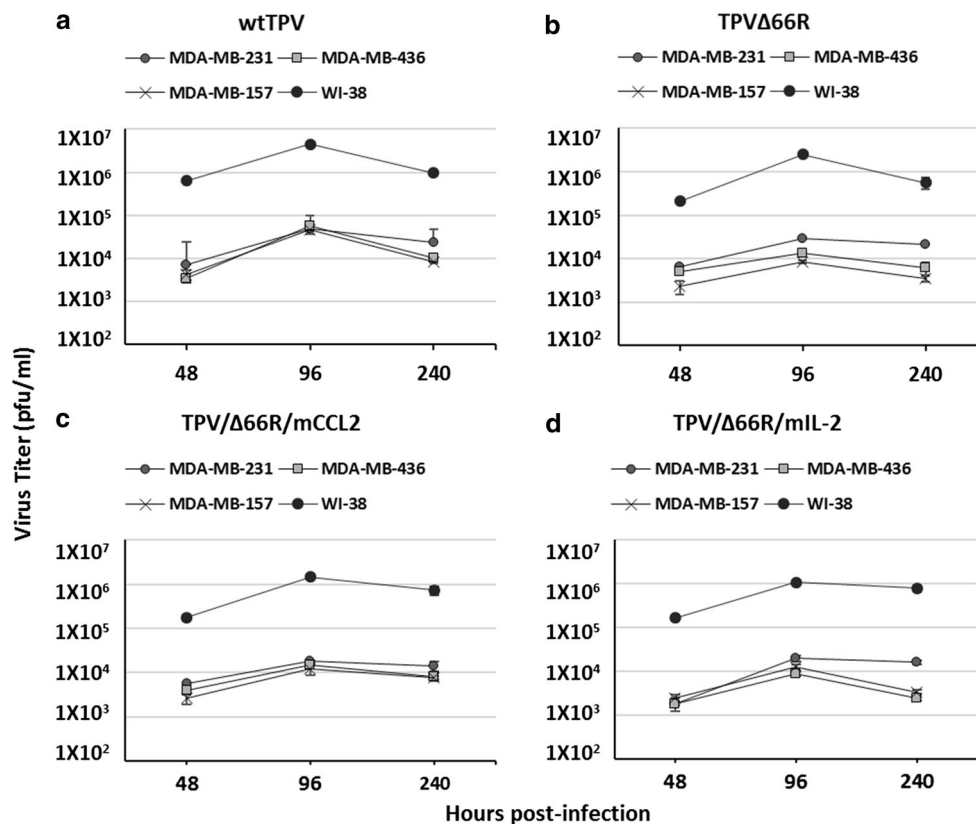


Fig. 1 Replication of tanapoxvirus recombinants in human triple negative breast cancer cells in vitro. The ability of tanapoxvirus (TPV) recombinants to replicate in various human cell lines including human fetal lung fibroblasts (WI-38) and human triple negative breast cancer cells (MDA-MB-231, MDA-MB-436, and MDA-MB-157) is determined by infecting cells at 0.1 MOI and determining the total virus titer at 48, 96 and 240 h postinfection (hpi). All TPV recombinants: **a** wild-type (wt) TPV, **b** TPV/ Δ 66R, **c** TPV/ Δ 66R/

mCCL2, and **d** TPV/ Δ 66R/mL-2 showed comparable replication in both WI-38 and human TNBC cells and destroyed most of the cells by 240 hpi in all wells. Deletion of 66R ORF slowed down the viral replication significantly ($p < 0.5$; Student's *T* test), and the viral titers of TPV/ Δ 66R were significantly lower than the wtTPV in all cells. Values are expressed as the mean plaque forming units (pfu)/ml (\pm SD) from triplicate experiments

very similar to TPV/ Δ 66R. All the viruses showed comparable levels of viral replication and increase in the titer of progeny virus in both WI-38 cells and human TNBC cells. These results confirm that wtTPV and all TPV recombinants can optimally replicate under favorable conditions.

TPV recombinants kill human triple negative breast cancer cells, in vitro

After investigating the replicability of TPV recombinants, we tested their cell killing ability in human TNBC cells. Infection of MDA-MB-157 cells with all TPV recombinants at 0.1 MOI resulted in a significant reduction in the cell viability at 240 hpi ($p < 0.05$) (Fig. 2a). Similarly, MDA-MB-436 cells showed a significant loss of viability ($p < 0.05$) at 240 hpi, when infected with all TPV recombinants at 0.1 MOI (Fig. 2b). Every TPV recombinant reduced the cell viability significantly ($p < 0.05$) in MDA-MB-231 cells at 0.1 MOI dose of infection at 240 hpi (Fig. 2d). Viral replication and cell viability assays

in human TNBC cells led us to choose MDA-MB-231 cells for inducing tumor xenografts in nude mice for the tumor virotherapy experiment due to three major reasons: (a) All TPV recombinants could replicate and kill MDA-MB-231 cells efficiently, (b) MDA-MB-231 cells are known to be tumorigenic in a nude mouse model [34, 35], and (c) CCL2 has been shown to promote survival and metastasis of MDA-MB-231 cells and we intended to study the effect of mCCL2 expressed by TPV recombinant on the survival and metastasis of these cells [36]. This prompted us to test the effect of TPV infection on the cell viability of MDA-MB-231 cells at a high dose of infection (5 MOI) and at 96 hpi time point. All TPV recombinants, except TPV/ Δ 66R induced a significant reduction in cell viability in MDA-MB-231 cells at 5 MOI at 96 hpi (Fig. 2c). Although TPV/ Δ 66R showed a reduced replicability as compared to the wtTPV, it was capable of significantly reducing the cell viability of MDA-MB-231 cells at both 0.1 and 5 MOI, by 240 hpi (Fig. 2c, d). TPV appears to reduce the cell viability of MDA-MB-231 cells in a dose-dependent manner.

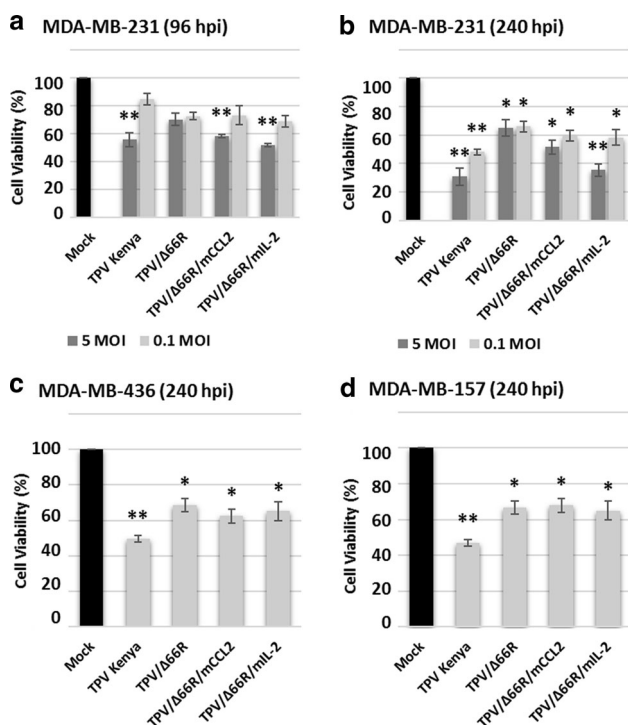


Fig. 2 Effect of TPV recombinant viruses on cell viability of human triple *negative* breast cancer. Human triple *negative* breast cancer (TNBC) cells MDA-MB-231, MDA-MB-436 and MDA-MB-157 were cultured in 96-well plate and either mock infected or infected with wild-type tanapoxvirus (TPV) or TPV/Δ66R or TPV/Δ66R/mCCL2 or TPV/Δ66R/mIL-2. **a, b** MDA-MB-231 cells were infected at 0.1 and 5 MOI, and cell viability was determined at 96-h postinfection (hpi) and 240 hpi using the CCK-8 assay. **c** MDA-MB-436 and **d** MDA-MB-157 cells were infected only at 0.1 MOI, and cell viability was determined at 240 hpi. All TPV recombinants significantly reduced the cell viability in all three TNBC cells at 240 hpi when infected with 0.1 MOI, in vitro ($p < 0.5$, One-way ANOVA). TPV recombinant reduced the cell viability in a dose-dependent manner, as all viruses reduced the viability of MDA-MB-231 cells significantly at 96 hpi when infected at 5 MOI but failed to do the same at 0.1 MOI. Values are expressed as the mean percentage loss in cell viability as compared to the mock group (\pm SD) from triplicate experiments

Mouse CCL2 does not promote survival of MDA-MB-231 cells in culture

Human CCL2 has been shown to promote the survival of MDA-MB-231 cells through Smad3 protein and p42/44 mitogen-activated protein kinase-dependent mechanisms [36]. Mouse CCL2 protein shows 55% homology with the human CCL2; however, to our knowledge, the cross-species effect of mCCL2 has not been studied on the survival of MDA-MB-231 cells. We investigated the effect of recombinant (r) mCCL2 by incubating MDA-MB-231 cells in serum-free medium without or with 10, 100 and 100,000 ng/ml of rmCCL2 for 24 h and determined the cell viability using the CCK-8 reagent as described earlier. The rmCCL2 did not promote survival of MDA-MB-231 cells

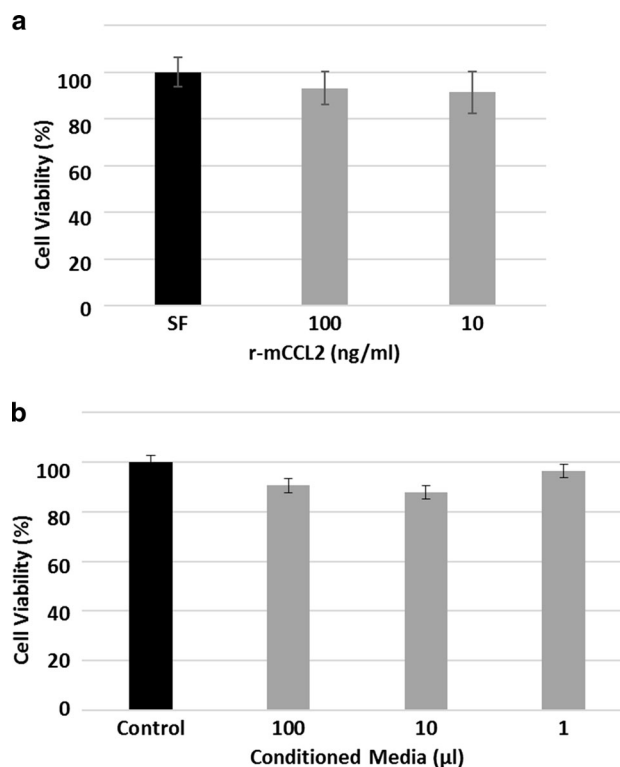


Fig. 3 Mouse CCL2 does not promote survival of MDA-MB-231 cells. **a** MDA-MB-231 cells were incubated in serum-free medium in the absence or presence of 10, 100 or 100,000 ng/ml recombinant mouse (m) CCL2 for 24 h, and percentage decrease in cell viability was calculated as compared to the mock. **b** MDA-MB-231 cells were incubated in control conditioned (100 μl) or CCL2 conditioned medium (1, 10, 100 μl) for 24 h, and percentage decrease in cell viability was calculated as compared to the mock, using CCK-8 assay kit. Values are expressed as mean (\pm SD). Error bars represent standard error

at all the dosages tested, in vitro (Fig. 3a). Similarly, the effect of mCCL2 expressed by TPV/Δ66R/mCCL2 was also investigated. The CCL2 conditioned medium was prepared after infecting OMK cells with TPV/Δ66R/mCCL2 that contained mCCL2. The control conditioned medium prepared similarly after infecting OMK cells with TPV/Δ66R which had no transgene inserted into its genome, but *66R* gene deleted was used to treat MDA-MB-231 cells (100 μl per well) in the control well. Like rmCCL2, mCCL2 expressed by TPV/Δ66R/mCCL2 also did not promote the survival of MDA-MB-231 cells when incubated with 1, 10 and 100 μl of CCL2 conditioned medium, in vitro as tested by the cell viability assay (Fig. 3b).

Tumor virotherapy of MDA-MB-231 xenografts in nude mouse

Subcutaneous tumor xenografts were induced in athymic nude-*Foxn1*tm mice by injecting MDA-MB-231 cells. Tumor xenografts reached a volume of 50 ± 5 mm³ in

2–3 weeks after injecting MDA-MB-231 cells when the mice were randomly assigned to either a mock or one of the virotherapy groups and tumors were injected accordingly. Complete results of tumor virotherapy are shown in Fig. 4. TPV/ Δ 66R/mCCL2 (Fig. 4c) and TPV/ Δ 66R/mIL-2

(Fig. 4d) showed vigorous and sustained therapeutic effect and significantly reduced tumor volumes, starting at day 16 posttreatment and kept the tumor volumes significantly lower as compared to the mock-injected groups throughout the course of virotherapy until 36-day posttreatment

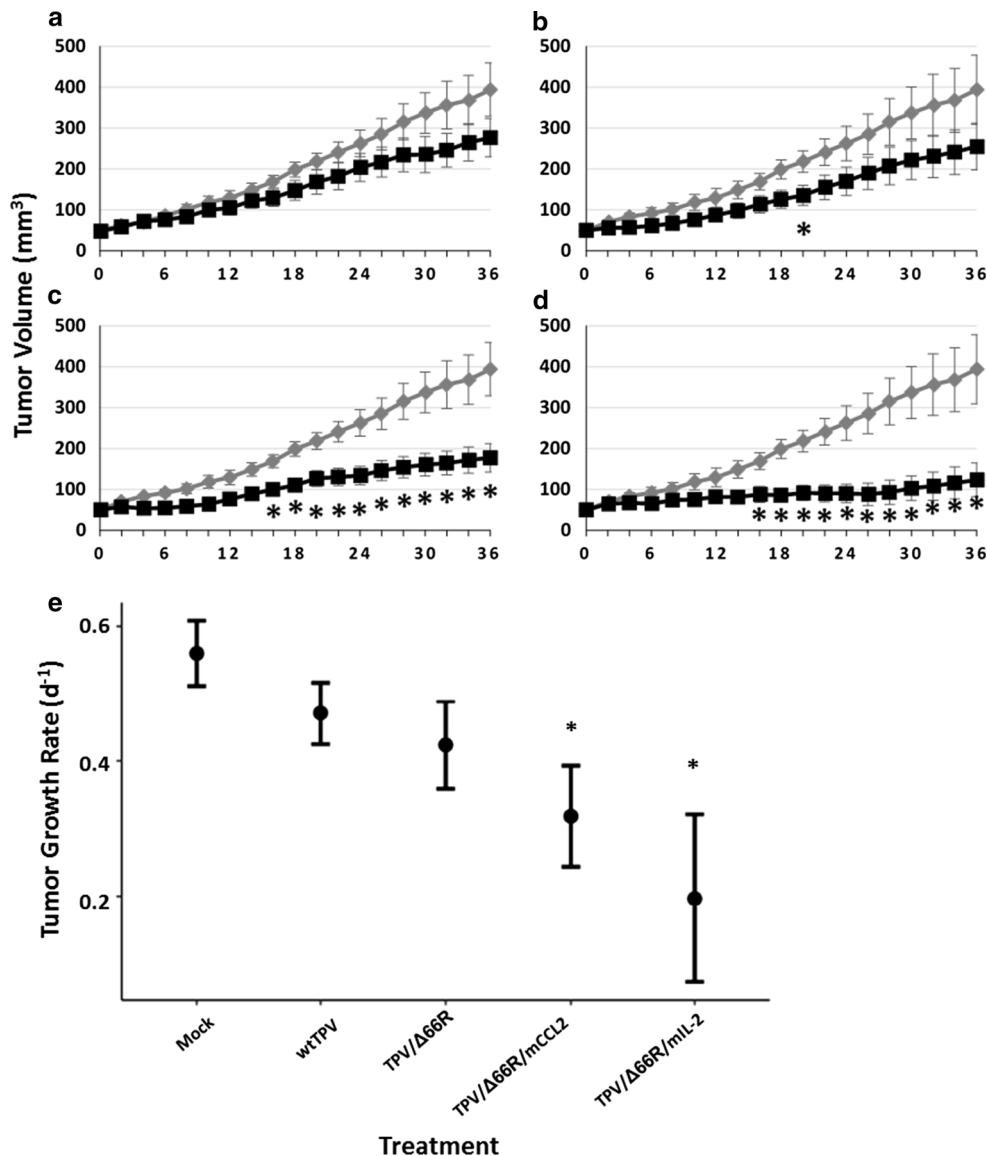


Fig. 4 Tumor virotherapy. Tumor volume analysis. Tumors were induced by subcutaneous injection of 5×10^6 MDA-MB-231 cells onto the dorsal surface (*inter-scapular region*) of athymic nude mice (each group $n = 5$ mice). Mice were randomly segregated into the control or experimental groups when tumor size reached 50 ± 5 mm³. In each graph the y-axis is tumor volume (mm³), and the x-axis is time (days post-virotherapeutic injection). A single mock injection containing 100 μ l of vehicle only or recombinant virus was administered at day 0, and tumor volume was measured at 2-day intervals. Tumor volume was calculated using the formula (length) \times (width) \times (height) \times ($\pi/6$). Average tumor volume is shown (black filled squares for each experimental group). Bars show the standard error of the mean (± 1 SEM). Points indicated with an asterisk (*) are significantly reduced from the control ($p < 0.05$). (a-

k) Mock virotherapeutic injection (vehicle only, gray diamonds). This is the group to which all experimental groups were compared to test for OV virotherapeutic effect upon average tumor volume. **a** wtTPV; **b** TPV/ Δ 66R; **c** TPV/ Δ 66R/mCCL2; **d** TPV/ Δ 66R/mIL-2. **e** Tumor growth rate analysis. Tumor growth (k) was estimated as $k = \log(\text{Vol}_t/\text{Vol}_0)/t$ for each mouse, where Vol_t and Vol_0 is the tumor volume on day t and day 0, respectively. We then used one-way ANOVA to test whether tumor growth rate (k) differed among treatments. We used planned contrasts to test whether tumor growth rate in the mock group differed from TPV treatment groups. Tumor growth rate in TPV/ Δ 66R/mCCL2 and TPV/ Δ 66R/mIL-2 treatment groups was significantly lower than the mock group ($p < 0.05$), as shown indicated by asterisk (*). All analyses were performed using R 3.3.2

($p < 0.05$). The maximum difference between the average tumor volumes between the mock-injected group and the two virotherapy treatment groups (TPV/ $\Delta 66R/mCCL2$ and TPV/ $\Delta 66R/mIL-2$) was on day 36 posttreatment. The average tumor volumes for TPV/ $\Delta 66R/mCCL2$ - and TPV/ $\Delta 66R/mIL-2$ -treated groups were 216.30 and 259.69 mm³ lower than the average tumor volume of the mock-injected group, respectively, on day 36 posttreatment. wtTPV (Fig. 4a)- and TPV/ $\Delta 66R$ (Fig. 4b)-treated tumors were relatively smaller than mock-injected tumors but failed to achieve statistical significance, except TPV/ $\Delta 66R$ (Fig. 4b)-treated tumors showed a significantly lower average tumor volume only at 20 days posttreatment ($p < 0.05$). The average tumor volume of TPV/ $\Delta 66R$ (Fig. 4b)-treated tumors was 82.93 mm³ lower than the average tumor volume of the mock-injected tumors, on day 20 posttreatment. The average tumor volume differences against the mock-injected tumors for wtTPV- and TPV/ $\Delta 66R$ -treated tumors were 117.34 and 139.03 mm³, respectively, on day 36 posttreatment.

Tumor growth rate analysis

On an average tumor volume increased by 5.60% per day in the mice treated with mock injection but only by 1.97% per day in the TPV/ $\Delta 66R/mIL-2$ -treated mice (Fig. 4e). The mean tumor growth rate was significantly lower than in the mice treated with mock injection for the animals treated with TPV/ $\Delta 66R/mCCL2$ ($F_{1, 20} = 4.93$, $p = 0.038$) and TPV/ $\Delta 66R/mIL-2$ ($F_{1, 20} = 11.14$, $p = 0.003$). Mean tumor growth rate in the wtTPV- or TPV/ $\Delta 66R$ -treated mice was not significantly lower than in the mice treated with mock injection (wtTPV: $F_{1, 20} = 0.68$, $p = 0.421$; TPV/ $\Delta 66R$: $F_{1, 20} = 1.58$, $p = 0.224$). Tumor growth rate did not differ significantly between the TPV/ $\Delta 66R/mCCL2$ treatment and the TPV/ $\Delta 66R$ treatment ($F_{1, 20} = 0.93$, $p = 0.346$), but it was significantly lower in the TPV/ $\Delta 66R/mIL-2$ treatment than in TPV/ $\Delta 66R$ -treated mice ($F_{1, 20} = 4.33$, $p = 0.05$).

Histopathological observations

There were characteristics that were present in all groups although to different degrees between the groups; these are presented in Table 1. The calculated areas of histo-sectioned tumor (the mid-section area) varied between and within each experimental group; however, although there was no statistically significant difference between the experimental groups and the mock control group in terms of section area, there was a clear trend with the mock group being the largest and other groups smaller. There appeared to be a clear reduction in mitotic index between the mock control and the treatment groups (Table 1), but this was not

seen to be statistically significant, except for the TPV/ $\Delta 66R/mIL-2$ -treated group ($p < 0.05$). Necrosis was common in all groups and presented as an aggregated area of cellular degeneration which extend to over 40% of the tumor mass in some cases. A specific characteristic of TPV/ $\Delta 66R/mIL-2$ -treated group was not seen in other groups with the isolated degenerating tumor cells that were present throughout the main body of viable neoplastic cells; these point areas of cell death were in addition to major areas of necrosis that were present in all groups.

There was a host cellular response in all groups, but there were clear differences between the groups in the type of host cell present in the capsule and in the degree of invasion of host cells into the tumor tissue. Although there was a host cellular response in all animals, including the mock controls, in the latter the cells tended to remain outside the tumor itself. All groups presented with a varying degree of fibrosis in the tumor capsule but TPV/ $\Delta 66R/mCCL2$ - and TPV/ $\Delta 66R/mIL-2$ -treated groups showed a relatively thinner fibrous tumor capsule. The most obvious clear invasion of inflammatory deep into the tumor tissue was seen only in the TPV/ $\Delta 66R/mIL-2$ -treated group, where the host inflammatory cells present deep into the tissues had the morphology of a small mononuclear lymphoid elements. In the wtTPV, TPV/ $\Delta 66R$ - and TPV/ $\Delta 66R/mCCL2$ -treated groups, there was an invasion of host inflammatory cells into the edges of the tumor reaching about 3–4 cells deep from the edge of the mass. However, in the TPV/ $\Delta 66R/mIL-2$ -treated group, the invading inflammatory cells (in this case almost uniquely lymphoid in form) reached deep into the tissues.

Discussion

In this study, TPV recombinants showed comparable replicability in vitro as evident by a substantial increase in the viral titers in infected human TNBC cells and significantly reduced their cell viability (Figs. 1; 2). These results showed that TPV can effectively kill TNBC cells merely through cell lysis in a dose-dependent manner, in the absence of a synergistic input in the form of antiviral immune responses. TPV/ $\Delta 66R/mCCL2$ (Fig. 4c) and TPV/ $\Delta 66R/mIL-2$ (Fig. 4d) were the most effective virotherapeutics among all TPV recombinants in vivo, in nude mice. CCL2 was first identified as a monocyte chemoattractant protein but can attract a wide array of immune cells such as monocytes, T lymphocytes, NK cells, dendritic cells and mast cells [18–20]. Similarly, IL-2 can promote immune responses mediated through T lymphocytes, macrophages and NK cells and play a critical role in differentiation and maturation of T cells [25–27]. The mCCL2 and mIL-2 expressed by TPV recombinants induced strong anticancer

Table 1 Histological analysis of tumors

Group	Mitotic index ^a	Capsular fibrosis ^c	Degree of pleomorphy ^d	Cell type in host cell response	Extent of cellular response in capsule ^e	Extent of host cell invasion into the tumor
Mock	3.1 ± 0.9	+++	+	Mixed	+++	Minimal
Wild-type TPV	2.8 ± 0.8	++	+	Mixed	+++	Edges only
TPV/Δ66R	2.0 ± 0.8	++	++	Mixed	++	Edges only
TPV/Δ66R/mCCL2	1.3 ± 0.9	+	+++	Mixed	++	Edges only
TPV/Δ66R/mIL-2	0.4 ± 0.2 ^b	+	+++	Mononuclear	+++	Deep invasion

^a Estimated as the number of mitoses per 100 cells from an observation of 10 different tumor cell dominant areas in the tumors selected at random

^b In a comparative analysis of each test group with the mock group, only the group TPV/Δ66R/mIL-2 was statistically significantly different ($p < 0.05$) from the control

^{c,d,e} Capsular fibrosis, degree of pleomorphy and extent of cellular response in tumor capsule were assessed using a semiquantitative system (normal –; minor changes +; moderate changes ++; extensive changes +++)

innate immune responses and enhanced the therapeutic efficacy of TPV significantly in the experimental nude mouse model.

Histopathological analysis of MDA-MB-231 tumor xenografts revealed that all tumors showed pleomorphic cells (Fig. 5a); however, the degree of pleomorphism differed among different treatment groups (Table 1). All tumor groups also showed areas with intact tumor cells (Fig. 5b) and necrotic foci, but the treatment groups had major areas of necrosis (Fig. 5c). Additionally, focal necrotic cells were seen in the TPV/Δ66R/mIL-2-treated tumors (Fig. 5j, k). Necrotic cell death in tumors correlated with tissue characteristics like vacuolation (Fig. 5l). All tumors clearly invoked a host response in nude mice where the TPV/Δ66R/mIL-2-treated group showed the most specific and significant host response. The TPV/Δ66R/mIL-2-treated tumors showed a robust mononuclear cell response where these cells infiltrated deep into the tumor capsule (Fig. 5e), while other tumor groups showed a mixed cellular response (Fig. 5f, h). Capsular infiltration in TPV/Δ66R/mCCL2-treated tumors was not as deep as TPV/Δ66R/mIL-2-treated tumors, but mast cells were found in the TPV/Δ66R/mCCL2-treated tumor capsules (Fig. 5g), indicating that mCCL2 expressed by the recombinant virus attracted the immune cells to suppress the tumor growth. Mast cells play a pleiotropic role in tumors and have shown both tumor promoting and antitumor effects [37]. It is likely that the effect of TPV/Δ66R/mCCL2 on the tumor microenvironment (TME) played an important role in reducing tumor growth efficiently as host immune cells were found around the tumor but did not invade the tumor capsule. The presence of tumor cells in draining lymphatics in TPV/Δ66R/mCCL2-treated group

indicates that mCCL2 expressed by the virus might be promoting the metastasis of tumor (Fig. 5i); however, no metastasis was found in the lung tissue (data not shown). Although some of the sublines of MDA-MB-231 cells have shown the ability to form secondary tumors specifically in lungs, the cells used in our experiment may or may not have the required the set of genes for establishment of secondary tumors in lungs [38].

The CCL2 attracts monocytes to tumors that differentiate into macrophages upon activation either into antitumor, inflammatory phenotype (M1) or pro-tumor, immunomodulatory (M2) phenotype, depending on the signaling factors. Pro-inflammatory signals like IFN- γ polarize activated macrophages to cytotoxic M1 phenotype [39]. IFNs are critical players of the host antiviral immune response [40] and expression of CCL2 by an engineered virus can attract monocytes to the tumor site and increased IFN levels in response to viral infection can possibly convert macrophages into the M1 phenotype.

In conclusion, TPV appears to be a suitable OV candidate that can kill human TNBC cells through direct cell lysis, following infection and induction of antitumor innate immune response. Among TPV recombinants tested, TPV/Δ66R/mCCL2 and TPV/Δ66R/mIL-2 have shown to suppress the growth of MDA-MB-231 xenografts significantly and histological analysis of tumors provides preliminary indications that the effect was mediated through induction of anticancer immunity. Although there were no statistically significant differences between the mock-injected and TPV/Δ66R/mCCL2-treated groups observed in the histological analysis, where only TPV/Δ66R/mIL-2 induced prominent and characteristically distinct histological changes, both TPV/Δ66R/mCCL2- and TPV/Δ66R/mIL-2-

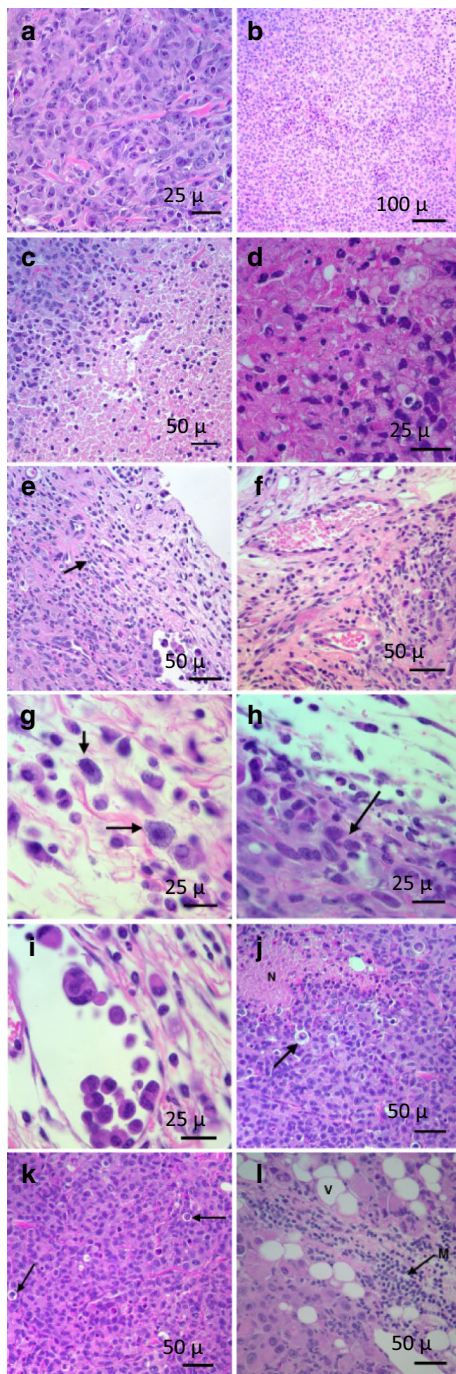


Fig. 5 Histological analysis of tumors. **a** H&E stained tumor showing pleomorphic cells; **b** H&E stained tumor with areas of intact tumor cell in the mock group; **c**, **d** representative image of necrotic areas in TPV/ Δ 66R/mIL-2-treated tumors; **e** infiltration of mononuclear cells (indicated by *black arrow*) in the capsule of TPV/ Δ 66R/mIL-2-treated tumors; **f** mixed capsular cellular response in TPV/ Δ 66R-treated group; **g** mast cells (indicated by *black arrow*) present in the capsule of TPV/ Δ 66R/mCCL2-treated tumors; **h** mixed capsular cellular response in TPV/ Δ 66R-treated group, *arrow* indicating tumor border; **i** neoplastic cells present in the draining lymphatics in the tumor capsule of TPV/ Δ 66R/mCCL2-treated tumors; **j**, **k** H&E stained tumor with areas of necrosis (indicated with *letter N*) and focal tumor cell death (indicated with *black arrow*); **l** deep mononuclear cell (indicated by *letter M* and *black arrow*) infiltration and vacuolation (indicated by *letter V*) in TPV/ Δ 66R/mIL-2-treated tumors

Recruitment of immune cells by TPV/ Δ 66R/mCCL2 and TPV/ Δ 66R/mIL-2 around MDA-MB-231 tumor xenografts, in a nude mouse model shows that these two viruses induced antitumor immune responses along with direct tumor cell lysis, to achieve a sustained suppression of tumor growth throughout the course of virotherapy.

Acknowledgements We are grateful to Dr. Chris Fisher, Dr. Sandhya Hasure and Farzad Razi for editorial comments. This study was partially supported by a National Institutes of Health Grant (1R15CA156262-01) and a Technology Development Award from Western Michigan University, awarded to KE.

Compliance with ethical standards

Conflict of interest Authors declare that they have no conflict of interest.

Human and animal rights This article does not contain any studies with human participants performed by any of the authors.

Informed consent No human subjects were used in the study.

Ethical approval All applicable international, national, and/or institutional guidelines for the care and use of animals were followed. Approval for involving mice in our study was obtained from Western Michigan University Animal Care and Use Committee (IACUC). The approval number is: IACUC protocol number 13-07-01. The policies set forth by the IACUC at Western Michigan University were followed while housing and treating the mice.

References

1. Siegel RL, Miller KD, Jemal A. Cancer statistics, 2016. *CA Cancer J Clin.* 2016;66:7–30.
2. Martelotto LG, Ng CK, Piscuoglio S, Weigelt B, Reis-Filho JS. Breast cancer intra-tumor heterogeneity. *Breast Cancer Res.* 2014;16:R48.
3. Meacham CE, Morrison SJ. Tumour heterogeneity and cancer cell plasticity. *Nature.* 2013;501:328–37.
4. Popa MA, Wallace KJ, Brunello A, Extermann M, Balducci L. Potential drug interactions and chemotoxicity in older patients with cancer receiving chemotherapy. *J Geriatr Oncol.* 2014;5:307–14.

treated groups showed lesser tumor capsular fibrosis as compared to the mock and other treatment groups (Table 1). The lower degree of capsular fibrosis in the TPV/ Δ 66R/mCCL2- and TPV/ Δ 66R/mIL-2-treated tumors could possibly be attributed to the mononuclear phagocytic cell response in the tumor vicinity which can lead to a rapid turnover of fibrotic tissue in the tumor capsule but the exact phenotype of mononuclear cells in the tumor vicinity needs to be determined to support this hypothesis [41].

5. Morris GJ, Naidu S, Topham AK, Guiles F, Xu Y, McCue P, et al. Differences in breast carcinoma characteristics in newly diagnosed African-American and Caucasian patients: a single-institution compilation compared with the National Cancer Institute's Surveillance, Epidemiology, and End Results database. *Cancer*. 2007;110:876–84.
6. Foulkes WD, Smith IE, Reis-Filho JS. Triple-negative breast cancer. *N Engl J Med*. 2010;363:1938–48.
7. O'Reilly EA, Gubbins L, Sharma S, Tully R, Guang MHZ, Weiner-Gorzel K, et al. The fate of chemoresistance in triple negative breast cancer (TNBC). *BBA Clin*. 2015;3:257–75.
8. Pol J, Kroemer G, Galluzzi L. First oncolytic virus approved for melanoma immunotherapy. *Oncoimmunology*. 2016;5(1):e1115641.
9. Pol J, Bloy N, Obrist F, Eggermont A, Galon J, Cremer I, et al. Trial watch: oncolytic viruses for cancer therapy. *Oncoimmunology*. 2014;3(6):e28694.
10. Suryawanshi YR, Zhang T, Essani K. Oncolytic viruses: emerging options for the treatment of breast cancer. *Med Oncol*. 2017;34:43.
11. Chan WM, McFadden G. Oncolytic poxviruses. *Annu Rev Virol*. 2014;1:119–41.
12. Downie AW, Taylor-Robinson CH, Caunt AE, Nelson GS, Manson-Bahr PE, Matthews TC. Tanapox: a new disease caused by a pox virus. *Br Med J*. 1971;1:363–8.
13. Monroe BP, Nakazawa YJ, Reynolds MG, Carroll DS. Estimating the geographic distribution of human Tanapox and potential reservoirs using ecological niche modeling. *Int J Health Geogr*. 2014;13:34.
14. Essani K, Bejcek BE, Seibert K. Yatapoxvirus. In: Tidona C, Darai G, editors. *The Springer index of viruses*. New York, NY: Springer New York. 2011. pp. 1511–21. doi:10.1007/978-0-387-95919-1_246.
15. Conrad SJ, El-Aswad M, Kurban E, Jeng D, Tripp BC, Nutting C, et al. Oncolytic tanapoxvirus expressing FliC causes regression of human colorectal cancer xenografts in nude mice. *J Exp Clin Cancer Res*. 2015;34:19.
16. Zhang T, Suryawanshi YR, Kordish DH, Woyczesczyk HM, Jeng D, Essani K. Tanapoxvirus lacking a neuregulin-like gene regresses human melanoma tumors in nude mice. *Virus Genes*. 2017;53(1):52–62.
17. Zhang Q, Yu YA, Wang E, Chen N, Danner RL, Munson PJ, et al. Eradication of solid human breast tumors in nude mice with an intravenously injected light-emitting oncolytic vaccinia virus. *Cancer Res*. 2007;67:10038–46.
18. Carr MW, Roth SJ, Luther E, Rose SS, Springer TA. Monocyte chemoattractant protein 1 acts as a T-lymphocyte chemoattractant. *Proc Natl Acad Sci USA*. 1994;91:3652–6.
19. Collington SJ, Hallgren J, Pease JE, Jones TG, Rollins BJ, Westwick J, et al. The role of the CCL2/CCR2 axis in mouse mast cell migration in vitro and in vivo. *J Immunol*. 2010;184:6114–23.
20. Xu LL, Warren MK, Rose WL, Gong W, Wang JM. Human recombinant monocyte chemotactic protein and other C-C chemokines bind and induce directional migration of dendritic cells in vitro. *J Leukoc Biol*. 1996;60:365–71.
21. Conti I, Rollins BJ. CCL2 (monocyte chemoattractant protein-1) and cancer. *Semin Cancer Biol*. 2004;14(3):149–54.
22. Lim SY, Yuzhalin AE, Gordon-Weeks AN, Muschel RJ. Targeting the CCL2-CCR2 signaling axis in cancer metastasis. *Oncotarget*. 2016;7:28697–710.
23. Monti P, Leone BE, Marchesi F, Balzano G, Zerbi A, Scaltrini F, et al. The CC chemokine MCP-1/CCL2 in pancreatic cancer progression: regulation of expression and potential mechanisms of antimalignant activity. *Cancer Res*. 2003;63:7451–61.
24. Parker JN, Meleth S, Hughes KB, Gillespie GY, Whitley RJ, Markert JM. Enhanced inhibition of syngeneic murine tumors by combinatorial therapy with genetically engineered HSV-1 expressing CCL2 and IL-12. *Cancer Gene Ther*. 2005;12:359–68.
25. Liao W, Lin J-X, Leonard WJ. IL-2 family cytokines: new insights into the complex roles of IL-2 as a broad regulator of T helper cell differentiation. *Curr Opin Immunol*. 2011;23:598–604.
26. Henney CS, Kuribayashi K, Kern DE, Gillis S. Interleukin-2 augments natural killer cell activity. *Nature*. 1981;291:335–8.
27. Han X, Wilbanks GD, Devaja O, Ruperelia V, Raju KS. IL-2 enhances standard IFN γ /LPS activation of macrophage cytotoxicity to human ovarian carcinoma in vitro: a potential for adoptive cellular immunotherapy. *Gynecol Oncol*. 1999;75:198–210.
28. Yong CSM, Dardalhon V, Devaud C, Taylor N, Darcy PK, Kershaw MH. CAR T cell therapy of solid tumors. *Immunol Cell Biol*. 2016. doi:10.1038/icb.2016.128.
29. Vacchelli E, Aranda F, Obrist F, Eggermont A, Galon J, Cremer I, et al. Trial watch: immunostimulatory cytokines in cancer therapy. *Oncoimmunology*. 2014;3:e29030.
30. Richmond A, Su Y. Mouse xenograft models vs GEM models for human cancer therapeutics. *Dis Model Mech*. 2008;1(2–3):78–82.
31. Cheers C, Waller R. Activated macrophages in congenitally athymic “nude mice” and in lethally irradiate mice. *J Immunol*. 1975;115:844–7.
32. Zhang T, Kordish DH, Suryawanshi YR, Essani K. Tanapoxvirus expressing interleukin-2 regresses human melanoma tumors by a T cell independent mechanism in mice. Le Bischenberg, Bischoffsheim (near Strasbourg), France: Poster session presented at: XXI International Poxvirus, Asfarvirus and Iridovirus Conference; 2016. pp. P10–2.
33. Mediratta S, Essani K. The replication cycle of tanapox virus in owl monkey kidney cells. *Can J Microbiol*. 1999;45:92–6.
34. Cai Z, Sanchez A, Shi Z, Zhang T, Liu M, Zhang D. Activation of toll-like receptor 5 on breast cancer cells by flagellin suppresses cell proliferation and tumor growth. *Cancer Res*. 2011;71:2466–75.
35. Lu X, Kang Y. Chemokine (C-C Motif) ligand 2 engages CCR2+ stromal cells of monocytic origin to promote breast cancer metastasis to lung and bone. *J Biol Chem*. 2009;284:29087–96.
36. Fang WB, Jocar I, Zou A, Lambert D, Dendukuri P, Cheng N. CCL2/CCR2 chemokine signaling coordinates survival and motility of breast cancer cells through Smad3 protein- and p42/44 mitogen-activated protein kinase (MAPK)-dependent mechanisms. *J Biol Chem*. 2012;287:36593–608.
37. Maciel TT, Moura IC, Hermine O. The role of mast cells in cancers. *F1000Prime Rep*. 2015;7:9.
38. Minn AJ, Gupta GP, Siegel PM, Bos PD, Shu W, Giri DD, et al. Genes that mediate breast cancer metastasis to lung. *Nature*. 2005;436:518–24.
39. Ivanova EA, Orekhov AN. Monocyte activation in immunopathology: cellular test for development of diagnostics and therapy. *J Immunol Res*. 2016. doi:10.1155/2016/4789279.
40. Muller U, Steinhoff U, Reis LF, Hemmi S, Pavlovic J, Zinkernagel RM, et al. Functional role of type I and type II interferons in antiviral defense. *Science*. 1994;264(5167):1918–21.
41. Lech M, Anders HJ. Macrophages and fibrosis: how resident and infiltrating mononuclear phagocytes orchestrate all phases of tissue injury and repair. *Biochim Biophys Acta*. 2013;1832(7):989–97.